Dynamics of Spin-Polarized Radical Pairs at the Solid/Solution Interface

Malcolm D. E. Forbes,* Shiyamalie R. Ruberu, and Katerina E. Dukes

Contribution from the Department of Chemistry, CB #3290, Venable and Kenan Laboratories, University of North Carolina, Chapel Hill, North Carolina 27599

Received January 20, 1994®

Abstract: Time resolved electron paramagnetic resonance (TREPR) spectroscopy has been used to investigate the magnetic and kinetic properties of monoradicals covalently bound to silicon oxide surfaces. Norrish I α-cleavage of aliphatic ketones and photoreduction of aromatic ketone n,π^* triplet states were used to produce the radicals. The ketones were anchored to the silica surface via a chlorosilane-terminated alkane chain. The aliphatic ketones were analogues of di-*tert*-butyl ketone, and the aromatic ketones were benzophenones connected at the ortho, meta, and para positions. A detailed description of the synthesis, attachment, and characterization procedures is given for all surface-anchored ketones. Comparison to TREPR spectra of similar structures in free solution shows that both radical pair (RPM) and triplet (TM) spin polarization mechanisms are affected by anchoring the molecules to the surface. Stronger TM polarization is observed in all cases, and increases in the line width are observed when the "tether" chain length is less than five carbon atoms. Longer tethers show line widths similar to those observed in free solution. Polar solvents at the interface also affect the ratio of RPM to TM polarization. The T_1 of the surface-bound radicals increases in some cases. These changes are discussed with respect to the rotational correlation time of the radicals and the "effective viscosity" at the interface. The ortho-alkylated benzophenone exhibits a long-lived EPR signal which may be due to a "photo-enol" type biradical, rather than monoradicals from the photoreduction process. Signals from the para-alkylated benzophenone show evidence for a spin-correlated radical pair (SCRP) at very early delay times.

Introduction

Organic photochemistry in heterogeneous media has become a major research topic.[1] Environments where diffusion is restricted, such as on surfaces or in the interior of zeolites and micelles, are of particular interest because they offer a higher "effective molarity" of reactants. This can significantly alter the course of chemical reactions and increase yields of products above that found in free solution.[2] It has been found in several laboratories that the lifetimes and reaction mechanisms of photoexcited organic molecules differ substantially from free solution when they are physically or chemically bound to surfaces.[3] Reactive intermediates produced from these excited states, such as free radicals and biradicals, have been observed mainly with luminescence techniques,[3a,4] or their presence has been inferred from product analysis.[5] These species can also show kinetic behavior and magnetic properties markedly different than those observed in free solution. For molecules incorporated into zeolite cavities, entirely new photochemical reaction pathways have sometimes been observed.[6]

In two recent preliminary publications from our laboratory, we reported time-resolved electron paramagnetic resonance (TREPR) spectra of mono- and biradicals confined to the solid/solution interface.[7] This technique provides fast time response and resolution, along with the high structural content of magnetic resonance spectroscopy. The observed radicals originate from the primary photochemical reactions taking place and are easily identified by spectral simulation. In all cases the phenomenon of chemically induced dynamic electron spin polarization (CIDEP) can be observed. The CIDEP pattern (emission vs absorption) depends greatly on the rotational motion, translational diffusion, and reencounter probabilities of the radicals and therefore may be useful in determining the role of the interface in the spin physics and chemistry of surface-bound radical pairs. The presence of CIDEP can also be used to investigate the kinetics and magnetic properties of the excited-state precursors, which can be difficult to study in detail by other physical methods.

The radical pair mechanism (RPM) and the triplet (TM) spin polarization mechanisms together constitute the usual definition of CIDEP.[8] The spin-correlated radical pair mechanism[9] (SCRP) exhibited by confined radical pairs and biradicals can be used to determine radical pair encounter rates and the distance dependent exchange interaction, J. Systems with restricted dimensionality

* Author to whom correspondence should be addressed.

® Abstract published in *Advance ACS Abstracts,* July 1, 1994.

(1) (a) Weiss, R. G.; Ramamurthy, V.; Hammond, G. S. *Acc. Chem. Res.* **1993**, *26*, 530. (b) Gehlen, M. H.; De Schryver, F. C. *Chem. Rev.* **1993**, *93*, 199. (c) Kamat, P. V. *Chem. Rev.* **1993**, *93*, 267. (d) Ramamurthy, V.; Eaton, D. F.; Caspar, J. V. *Acc. Chem. Res.* **1992**, *25*, 299. (e) Kalyanasundaram, K. *Photochemistry in Microheterogeneous Systems*; Academic Press: Orlando, FL, 1987.

(2) (a) Ramamurthy, V.; Corbin, D. R.; Johnston, L. J. *J. Am. Chem. Soc.* **1992**, *114*, 3870. (b) Buchanan, A. C., III; Biggs, C. A. *J. Org. Chem.* **1989**, *54*, 517. (c) Buchanan, A. C., III; Dunstan, T. J. D.; Douglas, E. C.; Poutsma, M. L. *J. Am. Chem. Soc.* **1986**, *108*, 7703.

(3) (a) Ramamurthy, V.; Sanderson, D. R.; Eaton, D. F. *J. Phys. Chem.* **1993**, *97*, 13380. (b) Kazanis, S.; Azarani, A.; Johnston, L. J. *J. Phys. Chem.* **1991**, *95*, 4430. (c) Wong, A. L.; Hunnicutt, M. L.; Harris, J. M. *J. Phys. Chem.* **1991**, *95*, 4489. (d) deMayo, P.; Natarajan, L. V.; Ware, W. R. In *ACS Symposium Series 278*; Fox, M. A., Ed.; American Chemical Society: Washington, DC, 1985; Chapter 1. (e) Thomas, J. K.; Wheeler, J. *J. Photochem.* **1985**, *28*, 285.

(4) (a) Turro, N. J.; Waterman, K. C.; Welsh, K. M.; Paczkowski, M. A.; Zimmt, M. B.; Cheng, C.-C.; Mahler, W. *Langmuir* **1988**, *4*, 677. (b) Turro, N. J. *Tetrahedron* **1987**, *43*, 1589. (c) Beck, G.; Thomas, J. K. *Chem. Phys. Lett.* **1983**, *94*, 553.

(5) (a) Turro, N. J.; Cheng, C.-C.; Mahler, W. *J. Am. Chem. Soc.* **1984**, *106*, 5022. (b) deMayo, P.; Nakamura, A.; Tsang, P. W. K.; Wong, S. K. *J. Am. Chem. Soc.* **1982**, *104*, 6824.

(6) Ramamurthy, V.; Lei, X.-G.; Turro, N. J.; Lewis, T. J.; Scheffer, J. R. *Tetrahedron Lett.* **1991**, *32*, 7675.

(7) (a) Forbes, M. D. E.; Myers, T. L.; Dukes, K. E.; Maynard, H. D. *J. Am. Chem. Soc.* **1992**, *114*, 353. (b) Forbes, M. D. E.; Dukes, K. E.; Myers, T. L.; Maynard, H. D.; Breivogel, C. S.; Jaspan, H. B. *J. Phys. Chem.* **1991**, *95*, 10547.

(8) (a) Trifunac, A. D.; Lawler, R. G.; Bartels, D. M.; Thurnauer, M. C. *Prog. React. Kinet.* **1986**, *14*, 43. (b) McLauchlan, K. A. In *Advanced EPR: Applications in Biology and Biochemistry*; Hoff, A. J., Ed.; Elsevier: New York, 1990; pp 345–369. (c) *Spin Polarization and Magnetic Effects in Radical Reactions*; Molin, Y., Ed.; Elsevier: New York, 1984; pp 224–242.

(9) (a) Closs, G. L.; Forbes, M. D. E.; Norris, J. R., Jr. *J. Phys. Chem.* **1987**, *91*, 3592. (b) Norris, J. R., Jr.; Morris, A. L.; Thurnauer, M. C.; Tang, J. *J. Chem. Phys.* **1990**, *92*, 4239. (c) Closs, G. L.; Forbes, M. D. E. *J. Phys. Chem.* **1991**, *95*, 1924. (d) Buckley, C. D.; Hunter, D. A.; Hore, P. J.; McLauchlan, K. A. *Chem. Phys. Lett.* **1987**, *135*, 307.

0002-7863/94/1516-7299$04.50/0

Scheme 1

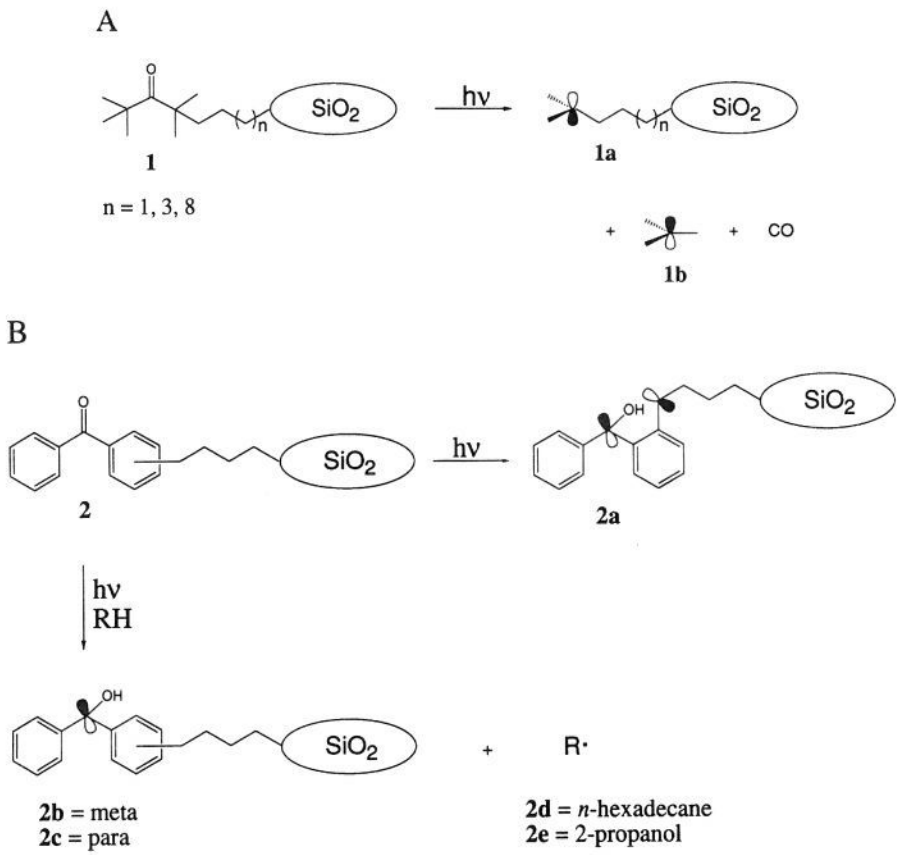

such as alkyl radicals on surfaces may also exhibit SCRP polarization as we shall demonstrate below. The primary signal decay pathway of CIDEP is spin relaxation rather than chemical reaction, and therefore information regarding molecular motion at the interface is available from the time dependence of CIDEP signals in this experiment. The line widths can be used to estimate the degree of motional narrowing of any anisotropic magnetic interactions that may be present. Examining all of the differences between surface and free solution CIDEP should allow an estimate of the rotational correlation times and the "effective viscosity" the bound radicals experience at the interface. In this paper we present a detailed investigation of the magnetic and kinetic properties of monoradicals covalently bound to silicon oxide and a qualitative analysis of the changes in the CIDEP mechanisms. We have modified the radical structure, the photochemical mechanism, and the solvent viscosity and polarity. In a separate paper, an analysis of TREPR spectra of surface-anchored, spin-correlated biradicals will be reported.

Results and Discussion

The systems we have investigated, along with their photochemistry, are shown in Scheme 1. We have chosen the standard Norrish I α-cleavage reaction and the intermolecular type II photoreduction processes for several reasons: (1) The solution photophysics and photochemistry of these systems are well understood, (2) the ketone functional group is inert toward the attachment procedure, (3) both types of reaction are known to produce radicals in reasonable yields, and (4) the starting materials are structurally simple and easily synthesized in a few steps. Excitation of linear, aliphatic tetramethyl ketones **1** is used to produce two alkyl radicals **1a** and **1b** (Scheme 1A), where **1b** is free to diffuse into the surrounding medium and **1a** remains tethered to the surface. Substituted benzophenones **2** are used to examine the type II photoreduction reaction (Scheme 1B). The H-atom abstraction by the bound ketone triplet state occurs from the freely moving solvent molecules. Here the chain length was not varied, but the position of attachment was changed from ortho to meta to para. Intermolecular photoreduction takes place for the meta and para isomers and leads to benzophenone ketyl radicals **2b** and **2c**, respectively, and solvent radicals **2d** and **2e**. The ortho isomer undergoes intramolecular H-atom abstraction to give 1,4-biradical **2a**. This difference in photochemical behavior will be elaborated upon in our discussion below. The solvents used for the type II reaction were 2-propanol, *n*-hexadecane, and sodium *n*-dodecylsulfate in water. Connection of the ketones to the silica gel is shown in Scheme 2. In each case attachment to the surface is accomplished by reaction of a chlorodimethylsilane group with the surface hydroxyl groups under basic conditions, following literature procedures which have been used to prepare reverse-phase chromatography column packing materials.[10] The silica gel has a very high surface area (BET measurement of 366 $m^2\ g^{-1}$) and is estimated to have 4.5 hydroxyl groups per nm^2 available as attachment sites for our silyl chlorides.[10b] The samples are washed and rinsed with several solvents of different polarities to remove physically adsorbed material, *vide infra*. After these washes and heating under vacuum for 24 h, the diffuse reflectance FTIR spectrum of the sample shows a strong band at 1685 cm^{-1}, assigned to the tetralkylated carbonyl group. The syntheses of the starting ketones are outlined in Scheme 3. Standard enolate/alkylation chemistry was used to produce the aliphatic keto alkenes (Scheme 3A), while the alkenyl-substituted benzophenones (BPs) were synthesized using Grignard and organolithium reagents followed by mild oxidation to the final products (Scheme 3B).

(10) (a) Shih-Hsien, H.; Fazio, S. D.; Tomellini, S. A.; Crowther, J. B.; Hartwick, R. A. *Chromatographia* **1985**, *20*, 161. (b) Berendsen, G. E.; de Galan, L. *J. Liquid Chromatogr.* **1978**, *1*, 403. (c) Berendsen, G. E.; Pikaart, K. A.; de Galan, L. *J. Liquid Chromatogr.* **1980**, *3*, 1437. (d) Berendsen, G. E.; de Galan, L. *J. Liquid Chromatogr.* **1978**, *1*, 561.

Scheme 2

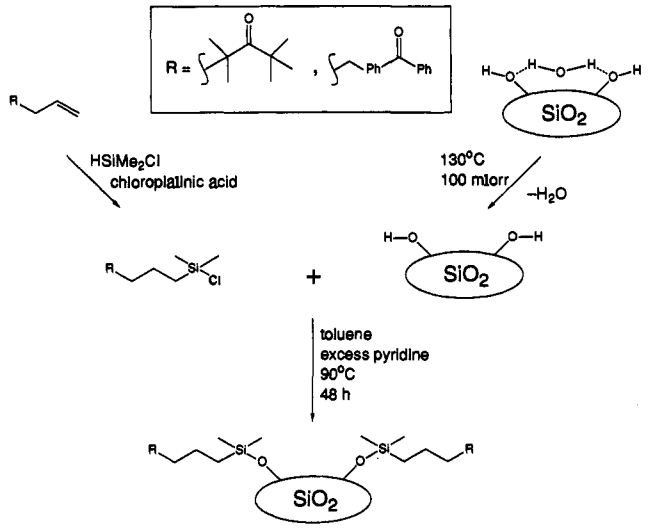

Scheme 3

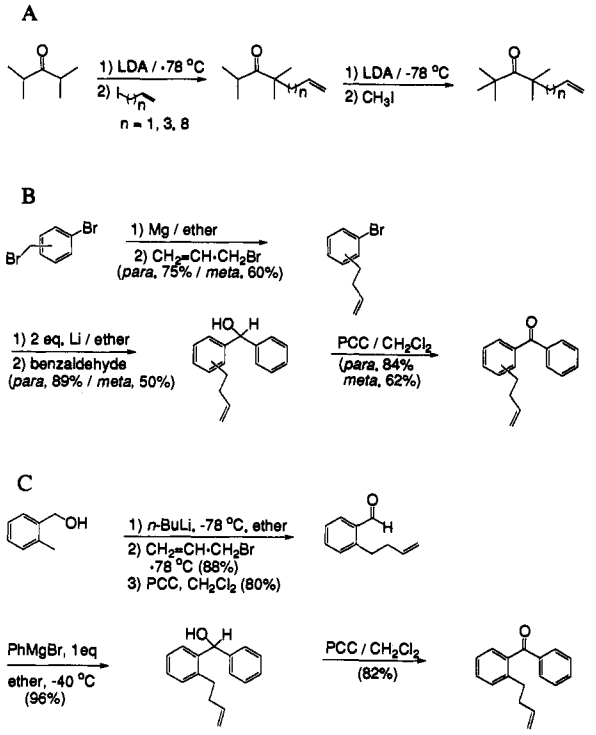

Impurities without terminal alkene moieties could be ignored because they do not undergo the hydrosilylation reaction and are later washed off the surface material. The samples for TREPR work are prepared by dispersing 1–2 g of modified silica gel in 50–100 mL of solvent. If less solvent is used, the resulting slurries are difficult to pump through the sample cell (0.5–1.0 mm path length) and become so opaque that scattering of the laser beam lowers the signal level substantially. The optical density of the slurries during pumping through the sample cell was extremely uniform at these concentrations. This was determined by running several different samples from different synthesis runs with different path lengths of flat cells and noting that the peak intensities were extremely reproducible in each experiment. Also, major changes in the optical density of the sample will affect the background signal from the laser beam hitting the walls of the cavity, which will in turn lead to base line shifts from the boxcar "light minus dark" gate subtraction process. This background level is extremely large for these samples because of scattering, but all of our experimental spectra show very flat base lines, so we conclude that there is not much change in the optical density of the sample during the TREPR scan. All samples were bubbled with dry nitrogen for 10 min before and during the collection of each spectrum.

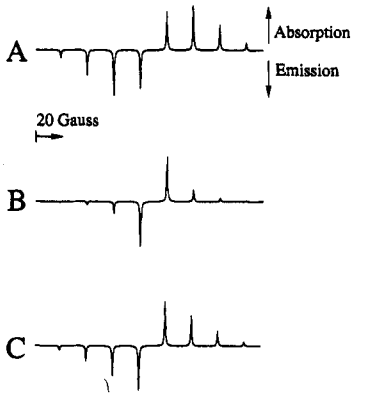

Figure 1. Simulated CIDEP spectra for a *tert*-butyl radical with an a_H value of 22.6 G for 9 equivalent H atoms and a *g*-factor of 2.0026. Simulations represent the radical pair mechanism only. The outermost transitions are very weak and have been cut off by the sweep width of 200 G: (A) 3D diffusion, the intensity scales with $(a_H)^{1/2}$; (B) 2D diffusion, the intensity scales with $\ln^{-2}(a_H)$; and (C) equally weighted sum of (A) and (B). See eq 1 and surrounding text for details.

Before presenting the data it will be instructive to begin with a discussion of the expected consequences of surface attachment for the spin polarization mechanisms of interest, i.e., RPM, TM, and SCRP polarization. Our experiments were originally prompted by a theoretical paper published in 1980 by Monchick,[11] who derived an expression for the magnitude of the RPM polarization P_{AB} when two radicals (A and B) are confined to diffusion in two dimensions. Comparisons with theoretical results for three-dimensional CIDEP[12] are summarized by eq 1.

$$P_{AB}(3D) \propto (a_H)^{1/2} \tag{1a}$$

$$P_{AB}(2D) \propto \ln^{-2}(a_H) \tag{1b}$$

The major difference between 2D and 3D CIDEP is the dependence on the electron-nuclear hyperfine coupling constant a_H, which is the off-diagonal element mixing singlet and triplet states of the radical pair.[13] In three dimensions P_{AB} scales with $(a_H)^{1/2}$, whereas Monchick's result for two-dimensional diffusion is that P_{AB} scales with $\ln^{-2}(a_H)$. Figure 1 shows a comparison of the two models using calculated spectra for a *tert*-butyl radical (radical A). The counter radical (radical B) contains no hyperfine interaction, and for clarity it is not shown. There are noticeable differences in the intensities between the two calculated spectra (Figure 1 (parts A and B for 3D and 2D CIDEP, respectively)). In particular the intensity of the centermost lines is greatly enhanced in the 2D case. Direct comparison of this result to our dataset may be difficult because the diffusion of the radicals in our experiments is really neither two- nor three-dimensional. The surface-bound member of the radical pair is restricted to a hemisphere with a plane defined by the surface and a radius defined by the overall length of the molecule. The unbound member is diffusing in the semiinfinite condition, the only restriction being the plane defined by the surface. Of course, this is a coarse approximation for both radicals considering the rough and porous nature of the silica gel surface. In a future publication, we will present Monte Carlo calculations of the conformational probabilities of surface-anchored alkyl chains as a function of

(11) Monchick, L. *J. Chem. Phys.* **1980**, *72*, 6258.
(12) Monchick, L.; Adrian, F. J. *J. Chem. Phys.* **1978**, *68*, 4376.
(13) With more than one hyperfine interaction the off-diagonal element becomes more complicated but still represents the local magnetic field difference between radicals A and B (assuming $\Delta g = 0$).

surface porosity and "roughness". Figure 1C shows a sum of the two effects, where each mechanism has been given equal weighting. The major change that might be observable in our experiments is the inversion of the relative intensities of the four innermost lines, which are also the most intense overall due to their degree of degeneracy. The appearance of such an inversion in our data would indicate that in fact some mixture of mechanisms is operative in these "quasi-2D" systems.

The above description applies to geminate radical pair polarization. In our experiments the concept of random (F-pair) polarization is somewhat different than in free solution. If we designate the geminate radicals as A and B, then in normal free solution random encounters take place from AA and BB pairs and from AB pairs when A and B originate from different geminate pairs. If *both* A and B are anchored close together on the surface, no random encounters are possible. When one is anchored, say the A radical, and the B radical is free to move, then no AA encounters are possible in the dilute condition. In fact, BB and AB random encounters may also be less likely based on the very low concentration of solution radicals expected in our experiments. We know approximately that there is one anchored ketone per 100 Å^2 of silica gel in our samples, which gives an effective ketone concentration in the slurry of about 30 mM.[7b] With an extinction coefficient at 308 nm of about 10 M^{-1} cm^{-1}, less than 0.1% of the ketones are absorbing the light per laser flash. With the large amount of scattering taking place, the actual number of ketones that become excited triplets and produce radical pairs must be very low indeed. Support for this also comes from the rather poor signal-to-noise ratios of the spectra reported here, although the turbulence of the slurry as it is being pumped through the microwave cavity also contributes to the noise. The probability of neighboring attachment sites producing radicals from the same laser flash is quite low. Under such conditions the polarization observed will be almost exclusively geminate pair CIDEP by the RPM. Random AB and BB encounters can be manipulated through solvent properties, which we now discuss.

There are several ways in which the solvent can influence the magnitude of the CIDEP phenomenon. The polarity of a solvent can influence the dynamics of charged radical pairs but tends to have little effect on neutral hydrocarbon radicals. If the radicals are small aliphatic molecules such as those shown in Scheme 1A, their high mobility (and/or volatility) may make hydrophobic effects difficult to observe. With larger radicals such as in Scheme 1B, confinement via hydrophobic effects or high viscosity is possible. The hydrophobic effect can be amplified through the use of surfactants on the solution side of the interface. This may have an effect on all three polarization mechanisms and will be examined in more detail below.

The magnitude of the RPM is strongly dependent on the viscosity the radicals experience.[14] In our experiments the unbound radical experiences the viscosity of the liquid at the interface, which is probably close to the bulk liquid viscosity. The surface-bound alkyl chain, on the other hand, has fewer translational and rotational degrees of freedom, and as a consequence the portion of the molecule closer to the surface behaves more like a solid than do those further away. Supporting evidence for this comes from molecular dynamics calculations by Klatte et al.,[15] which showed a substantial dynamical gradient for a C_8 alkyl chain with increasing distance away from a silica surface. Also, a study by Hommel and co-workers showed that chain length influenced the mobility of poly(ethyleneoxide) chains grafted to silica surfaces.[16] These studies and the present one strongly suggest that while the actual value of the viscosity of the liquid at the interface may not be very different from the bulk value, the surface-bound radical experiences an "effective viscosity" (or microviscosity) that is larger than the bulk liquid value. The concept of such a microviscosity has been suggested from studies of organic molecules solubilized in the interior of micelles and vesicles.[17] The mobility of the chains is governed by carbon–carbon single bond rotations whose rate constants can be expressed in terms of Arrhenius parameters E_a (activation energy) and A (frequency factor). The rotations in our surface-anchored chains can be slowed down by a change in A caused by increased friction with the surrounding medium or by a change in E_a from increased internal friction. A discussion of which mechanism is operative is outside the scope of this paper, but future studies of chain length effects in our systems may be useful in this regard.

It has been reported that the RPM in viscous solvents can be due to S–T^- mixing because the radicals can spend longer times in regions where the exchange interaction is comparable to the Zeeman energy at the magnetic field of interest.[18] McLauchlan and co-workers have reported expressions for the polarization intensities which are divided into nuclear spin dependent and independent parts.[19] The S–T^- mixing process will be a minor component contributing to the intensities of our spectra, usually masked by the presence of strong TM polarization (net absorptive or net emissive).

The TM depends on the magnetic properties and motion of the parent molecular ketone. The covalent bonds to the surface are far enough away that we can consider the populating rates into the molecular triplet by spin-orbit coupling from the excited singlet (k_{xx}, k_{yy}, and k_{zz}) and the zero-field splitting parameter, D, to be the same as for similar ketones in free solution. Additional assumptions are that (1) the α-cleavage rate is not affected by the attachment to the surface and (2) the spin relaxation times, T_1 and T_2, of the triplet state are altered only by changes in the molecular motion and not by interaction with other spins on the surface or in the bulk of the silica gel. Both of these assumptions seem valid when considering the insulating nature of the silicon oxide. Because the experiments are run at only one microwave frequency (X-band = 9.5 GHz), there is then only one molecular parameter that can change the magnitude of the TM: the rotational correlation time of the ketone, τ_c. It can alter the TM intensity in two ways: by changing (1) the spin–lattice relaxation time of the ketone triplet state and (2) the extent of rotational averaging of the zero-field splitting D. In a recent publication, we presented an analysis of the τ_c dependence of the TM for spin-polarized short biradicals in liquid solution, to which the reader is referred for further details.[20] At X-band, electron T_1's are close to their minimum value for small organic molecules tumbling in organic solvents with viscosities of about 1 cP. If the viscosity becomes lower, the T_1 value increases, but the dipolar interaction is more efficiently rotationally averaged, and so there is usually a decrease in the magnitude of the TM. The TM is maximized by moving τ_c toward the slow tumbling region. For our samples the parent ketone triplet is always anchored to the surface and experiences the higher effective viscosity discussed above. We therefore expect to see stronger TM polarization in most cases when the triplet is surface attached.

The SCRP polarization is normally encountered in biradicals,[21] confined radical pairs such as those incorporated in micelles,[9a] and in solutions of high viscosity.[9d] At the interface, only one of the radicals experiences a higher viscosity than the other, and it is not clear that this is an adequate condition for the observation of SCRPs within our time resolution. The silica gel used in these

(14) (a) Pedersen, J. B.; Freed, J. H. *J. Chem. Phys.* **1973**, *58*, 2746. (b) Goudsmit, G.-H.; Paul, H.; Shushin, A. I. *J. Phys. Chem.* **1993**, *97*, 13243. (c) Pedersen, J. B.; Hansen, C. E. M.; Parbo, H.; Muus, L. T. *J. Chem. Phys.* **1975**, *63*, 239.

(15) Klatte, S. J.; Beck, T. L. *J. Phys. Chem.* **1993**, *97*, 5727.

(16) Hommel, H.; Facchini, L.; LeGrand, A. P.; LeCourtier, J. *Euro. Polym. J.* **1978**, *14*, 803.

(17) Reference 1e, p 46.

(18) (a) Trifunac, A. D. *Chem. Phys. Lett.* **1977**, *49*, 457. (b) Kawai, A.; Obi, K. *J. Phys. Chem.* **1992**, *96*, 5701.

(19) (a) Buckley, C. D.; McLauchlan, K. A.; *Chem. Phys. Lett.* **1987**, *137*, 86. (b) Reference 8b, p 354.

(20) Forbes, M. D. E.; Ruberu, S. R. *J. Phys. Chem.* **1993**, *97*, 13223.

(21) Closs, G. L.; Forbes, M. D. E. In *Kinetics and Spectroscopy of Carbenes and* Biradicals; Platz, M. S., Ed.; Plenum: New York, 1990; p 51.

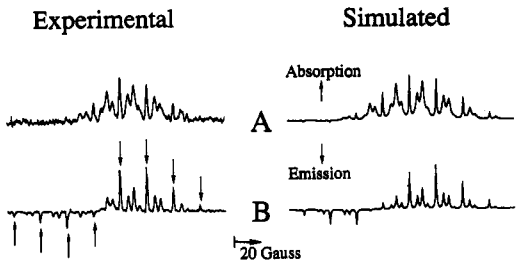

Figure 2. (A) Experimental and simulated TREPR spectra for the radical pair shown in Scheme 1A taken at a delay time of 0.4 μs in benzene. Radical **1a** hyperfines were 22.2 G for 6 equivalent H atoms and 17.8 G for 2 equivalent H atoms. Radical **1b** (*tert*-butyl) hyperfine values were 22.6 for 9 equivalent H atoms. Both *g*-factors were equal to 2.0026. Line widths (reported as fwhm throughout) are 3.0 G for radical **1a** and 1.0 G for **1b**. The ratio RPM:TM is 1:3.7. (B) Experimental and simulated TREPR spectra for the same radical pair at 0.4 μs in free solution (benzene). Hyperfine values are the same as in (A). The line width of the dimethylpentyl radical is 1.5 G, and the line width of *tert*-butyl radical is 1.0 G. The ratio RPM:TM is 1:1.3.

experiments is extremely porous, and it is possible that some radicals, when initially formed, are trapped for a short time until the freely moving radical can escape. This is an additional situation which can lead to SCRP polarization. We now turn our attention to the experimental data to see if the changes in the RPM, TM, and SCRP polarization mechanisms predicted above are observed.

A. Results for Norrish I α-Cleavage Reactions. A representative TREPR spectrum from the photochemical reaction outlined in Scheme 1A is shown in Figure 2A, with the same radical from a similar precursor in free solution shown for comparison in Figure 2B. The solvent in both spectra is benzene. The second radical, free to move into the solution after the α-cleavage reaction, is the *tert*-butyl radical in both cases, and its EPR transitions are identified in Figure 2 with arrows. The free solution experiment, when run in the presence of unmodified dry silica gel, shows essentially the same spectrum as in Figure 2B. Clearly, the inversion of the relative intensities of the centermost transitions is observed, but two types of simulations can account for this change (1) using a mixture of TM and RPM and (2) using a mixture of the 2D and 3D CIDEP results of Monchick and Adrian. Elucidation of the mechanism therefore remains inconclusive because of complications caused by the TM.

As we have pointed out in our preliminary reports,[7] the major differences between these spectra are the shift in the spin polarization mechanism from RPM to TM and an increase in the line width of the surface-anchored radical by about 60%. The line width of the free solution radical remains unchanged from that in Figure 2B. As predicted above, the bound radical signal is broadened because the system is not quite in the solid state (close to the surface) nor is it in the liquid state (at the radical site itself). If the alkyl chain is made longer (more liquid-like), e.g., two more carbon atoms in the chain, then the line width of the bound radical returns to a value close to that observed in free solution.[7b] Attempts to extend this experiment to a ten carbon atom alkyl chain were unsuccessful. It has become a general osbervation in our laboratory that when the anchoring chain is as long as 10 carbon atoms, obtaining enough surface coverage to show even weak TREPR signals becomes difficult. We note that this result is in line with reverse-phase chromatography support technology, which clearly demonstrates that chains of up to 18 carbon atoms can be attached relatively easily, but only limited coverage is observed because the attached molecules sterically block the remaining sites.[22] We assume that for the longer chain lengths we have not been able to cover the SiO_2 surface with enough ketone to produce an observable TREPR signal with our sensitivity.

(22) Dorsey, J. G.; Dill, K. A. *Chem. Rev.* **1989**, *89*, 331.

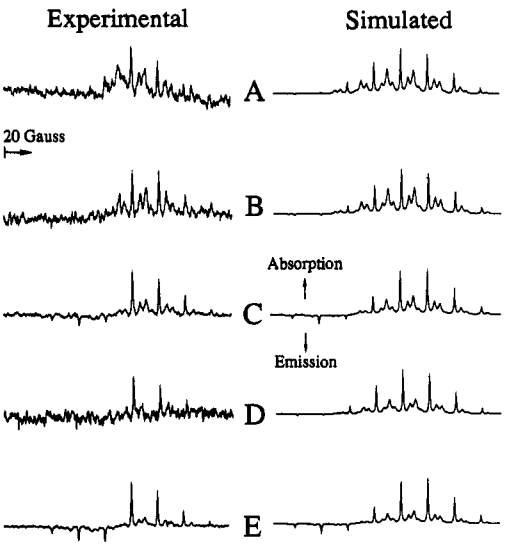

Figure 3. Left: Solvent dependence of X-band TREPR spectra for the radical pair **1a**/**1b** taken at a delay time of 1 μs. Right: Simulations using the parameters listed in the legend of Figure 2. The solvent systems (slurries) shown are (A) benzene, (B) methanol, (C) methanol/water (1:1), (D) water, and (E) 0.1M SDS in water. In all spectra the line width of radical **1a** is 2.8 G, and the line width of radical **1b** is 1.0 G, except in (D) where the line width of radical **1a** is 3.2 G: (A) RPM:TM = 1:5, (B) RPM:TM = 1:4, (C) RPM:TM = 1:2.2, (D) RPM:TM = 1:4, and (E) RPM:TM = 1:2.

A question arises as to the origin of the shift in the polarization mechanism from RPM to TM. Is it a decrease in the RPM or an increase in the TM? As noted by Monchick, restricted diffusion is generally going to increase encounter probabilities so that RPM should be stronger overall in two dimensions compared to three; therefore, it is difficult to rationalize a decrease in the magnitude of the RPM. As stated above for the TM, any increase in the viscosity at X-band is going to have a strong effect on this mechanism because it will in general lead to larger triplet T_1 values and less efficient averaging of the zero-field splitting. The increased line width already indicates that the motion is slower for the bound species, and since the parent ketone is a larger molecule than the radical it is a logical conclusion that the TM has been enhanced. We will return to a discussion of the RPM when the time dependence of these signals is presented.

Figure 3 shows the same system in five different solvent systems ranging in dielectric constant from that of benzene to water. By inspection it is apparent that there is a solvent dependence on the magnitude of the polarization mechanisms. The lifetimes of the photoexcited states can be affected by solvent polarity, but spin relaxation times and S–T intersystem crossing rate constants in ketones generally will be not be strongly affected. Since the viscosity is also different in each solvent system, changes in the RPM are difficult to assign exclusively to either a viscosity or polarity effect. With water or methanol, the poor signal-to-noise ratios also prevent us from drawing conclusions regarding these two effects. The spectra shown in Figure 3 are typically the sum of several scans. Because of the destructive photochemistry, sample lifetime prevents further averaging. In the case of water, the sample was extremely heterogeneous due to inefficient wetting of the surface material, and this made both pumping the sample and maintaining uniform optical density difficult. The attachment of alkyl groups makes the surface material waxy in appearance, and the wetting process upon initial preparation of the slurries is easily observable. In water the modified surface material becomes clumpy and tends to float on the surface of the solvent, indicating very different surface tension characteristics than in other solvent systems.

Attempts to observe SCRP polarization in these radicals by "trapping" the geminate pair for longer times using sodium dodecyl

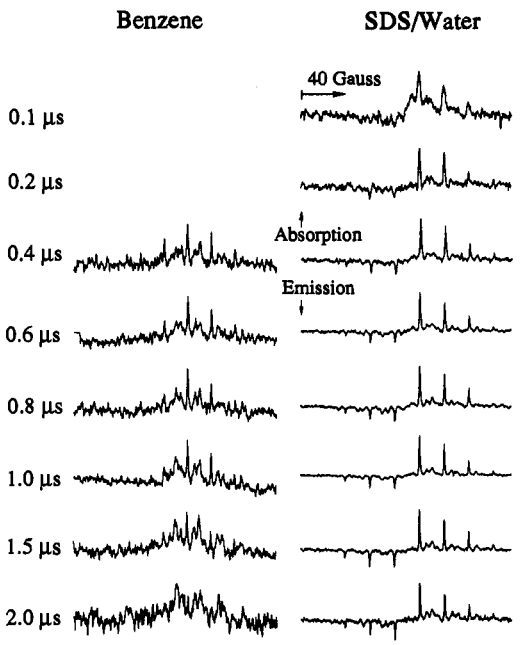

Figure 4. Left: Time dependence of X-band TREPR spectra for the radical pair from Scheme 1A in a benzene slurry. Right: Time dependence of the same radical pair in a water slurry that is 0.1 M in sodium-*n*-dodecyl sulfate.

sulfate (SDS) detergent molecules in the aqueous solution is shown in Figure 3E. The SCRP splitting pattern of emission/absorption for each hyperfine line is not observed. This result is not entirely surprising considering the high mobility of the unbound radical. In fact, if the experiment is run using the model system from Figure 2B in micellar solution (same radicals with no surface), SCRP polarization is not observed. It is estimated that the radical pair spends only tens of nanoseconds as an SCRP before exiting the micelle or undergoing geminate recombination. The exit rates of small organic radicals in SDS micelles have been measured by transient optical absorption[23] to be 6.6×10^6 s^{-1}, consistent with the fact that SCRP polarization in those micellar systems has not been observed by TREPR.[24] The actual structure we propose for our silica/SDS/water system will be discussed in more detail below.

It is interesting to note that the intensity ratio of the two radicals changes for each solvent system. This can be due to changes in the spin–lattice relaxation times of either radical, i.e., the T_1 of the surface radical decreases or that of the solution radical increases going down Figure 3. The line width of the surface radical changes very little in parts A–E. The solution radical could receive stronger RPM polarization by experiencing random encounters more easily than the surface radical. To investigate this further, the time dependence of the EPR signals in benzene and SDS/water were compared. The results are shown in Figure 4. In both solvent systems the surface radical polarization pattern does not change very much, although this is difficult to determine for the spectra taken in benzene except perhaps near the 1.0 μs delay time. Both radical signals in benzene decay at slightly different rates, to the point where at 2.0 μs the surface radical is actually more intense. Alkyl radicals in solution have lifetimes in the range of 10–100 μs, and those anchored to an insulating surface are expected to live even longer due to diffusion restrictions. There is a report of extremely long chemical lifetimes for free radicals confined to the interior of a zeolite.[25] Another consequence of the long lifetimes is the possibility of different products being formed compared to free solution. Product analysis for the surface systems could be accomplished by digestion of the photolyzed material in hot aqueous KOH, but for the aliphatic systems this was complicated by the volatility of the photoproducts once they are cleaved from the surface. Product analysis was more successful for the aromatic systems and will be discussed in more detail below.

The time dependence of the SDS/water system in Figure 4 shows clear differences from that in benzene. The polarization is stronger (good signal-to-noise ratio) for both mechanisms, yet at comparable delay times the RPM is stronger in SDS/water than in benzene. Additionally, the magnitude of the RPM polarization increases with time for the solution radical, while the RPM pattern of the surface radical shows only a minor increase with delay time. Since both radicals receive equal TM polarization at the time of formation of the geminate pair and geminate RPM polarization is produced within the first few nanoseconds, the growth of further RPM polarization must be dominated by random encounters. This is strong evidence in support of the hypothesis above that solution radicals will have a higher probability of random encounters than surface radicals. As noted above, the higher mobility of the solution radicals prevents observation of SCRP polarization, but there is another factor involved. With the rough surface of silica gel particles, the detergent molecules are unable to form highly organized assemblies such as monolayers, bilayers, or micelles right at the interface. As a result this system is expected to be much more disordered than a simple smooth SiO_2 surface. The detergent molecules are large and may not be able to get close enough to the surface to "trap" SCRPs long enough to be osberved by TREPR. It is interesting to note that the magnitude of the TM is not affected as much on going from benzene to SDS/water, even though the viscosity in the interior of an SDS micelle or monolayer is about an order of magnitude higher than that of water.[26] This observation suggests that the parent ketones are experiencing higher mobility in the silica/SDS/water system than in ordinary micelles. The disorder at the interface caused by the surface roughness will cause more water to be present there, lowering the viscosity. Moving, say, a few layers of solvent away from the interface, the solution becomes more ordered either by micelle formation or other aggregation. The α-cleavage reaction and the production of TM polarization both take place in regions of lower viscosity, while reencounters of random radical pairs may be influenced by the higher viscosity regions further away from the interface.

B. Results for Type II Photoreduction Reactions. The photoreduction of surface-anchored BP triplet states by hydrogen atom donor solvents (RH) as shown in Scheme 1B was studied. In this case the photochemistry is intermolecular and we expect that the polarization mechanisms should be strong functions of the solvent properties. The two radicals produced are the benzophenone ketyl radical and an alkyl radical from the solvent. We have anchored the BP to the surface through a four carbon atom chain connected ortho, meta, and para to the carbonyl group. Figure 5 shows the time dependence of the TREPR signals obtained from photoreduction of the para-connected alkyl BP in two different solvents, 2-propanol (Figure 5A) and *n*-hexadecane (Figure 5B). An immediately obvious feature of all of these spectra is that the TM is now the dominant polarization mechanism. Also, the line width of the surface-bound radical **2c** is quite large, while the solution radical (**2d** and **2e**) line width has also increased somewhat. The anchored BP triplet state is

(23) Cozens, Frances L.; Scaiano, J. C. *J. Am. Chem. Soc.* **1993**, *115*, 5204.

(24) Turro, N. J.; Paczkowski, M. A.; Zimmt, M. B.; Wan, J. K. S. *Chem. Phys. Lett.* **1985**, *114*, 561.

(25) (a) Kelly, G.; Willsher, C. J.; Wilkinson, F.; Netto-Ferreira, J. L.; Olea, A.; Weir, D.; Johnston, L. J.; Scaiano, J. C. *Can. J. Chem.* **1990**, *68*, 812. (b) Johnston, L. J.; Scaiano, J. C.; Shi, J.-L.; Siebrand, W.; Zerbetto, F. *J. Phys. Chem.* **1991**, *95*, 10018.

(26) (a) Shinitky, M.; Dianoux, A.-C.; Gitler, C.; Weber, G. *Biochemistry* **1971**, *10*, 2016. (b) Turro, N. J.; Tanimoto, Y. *Photochem. Photobiol.* **1981**, *34*, 157.

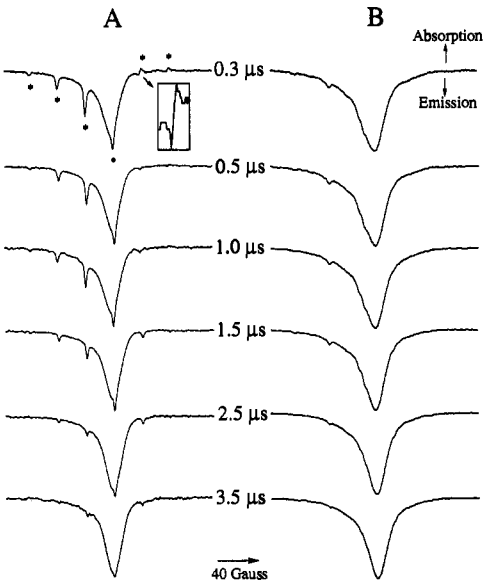

Figure 5. X-band time-resolved EPR spectra obtained at the delay times indicated for *p*-butylbenzophenone/silica system **2** in (A) 2-propanol (B) *n*-hexadecane. Asterisks denote the 2-propanoyl radical **2e**. The broad central line is assigned to radical **2c**. The inset displays a vertical expansion showing the SCRP polarization pattern.

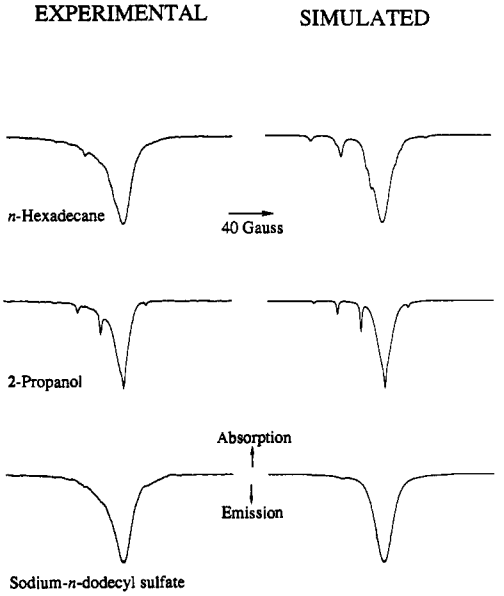

Figure 6. Experimental (left) and simulated (right) X-band TREPR spectra obtained at a 1.0 μs delay time during photolysis of *p*-butylbenzophenone anchored to SiO_2 in slurries using the solvents indicated.

Scheme 4

$$^3[BP] \xrightarrow[k_1]{RH} \underset{\text{(TM, SCRP)}}{BP\cdot/R\cdot} \xrightarrow{k_2} \underset{\text{(TM, RPM)}}{BP\cdot + R\cdot}$$

much larger than the aliphatic ketones from Scheme 1A. It is not surprising that it would tumble more slowly, which should lead to more TM. The difference in line widths of the two solution radicals in Figure 5 (parts A and B) can be attributed to the higher bulk solution viscosity of *n*-hexadecane over 2-propanol. Because the low field lines are more strongly emissive than the high field ones, there is some RPM present in both datasets. A novel feature of Figure 5A is the appearance of splittings (emissive/absorptive) in the high field lines at the very earliest delay time. This is shown in more detail in the inset of Figure 5. In the SCRP polarization each hyperfine line is split into a doublet having an emissive/absorptive (E/A) pattern. This occurs when radical pairs are in restricted environments where they experience limited diffusion, and the splitting between adjacent E/A doublets is equal to the exchange interaction or singlet–triplet energy gap $2J$. The splitting pattern seen here is evidence for the initial formation of a "trapped" radical pair at the interface, which then separates to regions where there is no longer any spin correlation. Scheme 4 outlines how these SCRPs can be produced and would only be observable at very early delay times. The initially formed radical pair (RP) has TM polarization from the parent ketone but quickly develops strong SCRP polarization. Since the concentration of RPs is fairly low at early times and the SCRP polarization is about an order of magnitude stronger than the TM[9a], some SCRP is observed. At later times, the concentration of separated free radicals with TM and RPM polarization is large and masks the small concentration of SCRPs. All that is required is that $k_2 > k_1$ in Scheme 4, which is likely to be the case because k_1 is known in solution to be about 3×10^6 s^{-1},[27] and even with very slow diffusion of solvent radicals away from the surface, k_2 should be an order of magnitude faster than this. We calculate the translational diffusion rate of the solvent radical in hexadecane to be 4.5×10^7 s^{-1} for a distance traveled of 40 Å. This is far enough away that the exchange interaction can be assumed to be zero, and this number is consistent with the argument presented above for SCRP observation at early delay times.

Simulations of representative spectra using literature values for hyperfine coupling constants and g factors[28] are shown in Figure 6 to illustrate the unambiguous assignment of the observed signals to the radicals depicted in Scheme 1B. It is clear from the *n*-hexadecane simulation that the line shape is no longer purely Lorentzian, which can be expected on moving to the slow motion region. Also shown is an attempt to observe SCRPs when SDS is present in an aqueous solution surrounding the surface. While there are signals at the right position for alkyl radicals from H-atom abstraction from SDS, the lines are so broad and the TM so dominant that no distinct SCRP polarization could be detected at any delay time.

Figures 7 and 8 show a comparison of these systems to the same structures in free solution. For the solution experiments the parent (unattached) *p*-but-1-en-4-ylbenzophenone was used, with a comparable concentration to that in the surface experiments. Figure 7 (parts A and B) shows the large change in the magnitude of the TM. To show the identity of the radicals and to resolve overlapping signals, Figure 7C shows the first derivative of the experimental *n*-hexadecane spectrum at 1.0 μs (top left spectrum in Figure 6A). The spectrum was collected in direct detection, but the derivative was obtained numerically. The alkyl radical transitions are now much better resolved. Figure 7D shows a numerically calculated first derivative of the simulation in Figure 7A. The agreement between the two derivative spectra in Figure 7 is very good and lends further support to the assignments, intensities, and line width changes. In Figure 8, the time dependence of each surface/solvent system is displayed next to the same system in free solution. It should be noted that the free solution spectra were obtained with larger concentrations of starting ketones, yet showed weaker signals than the surface spectra. For 2-propanol there is almost no TM in free solution, and even the ketyl radical shows strong RPM polarization (emissive/absorptive). Also, the solvent radical in the 2-propanol solution appears to decay with approximately the same time constant in both surface and free solution cases, but there is a

(27) Scaiano, J. C.; Abuin, E. B.; Stewart, L. C. *J. Am. Chem. Soc.* **1982**, *104*, 5673.

(28) (a) Greatorex, D.; Hill, R. J.; Kemp, T. J.; Stone, T. J. *J. Chem. Soc., Faraday Trans. I* **1974**, *70*, 216. (b) Paul, H.; Fischer, H. *Helv. Chim. Acta* **1973**, *56*, 1575. (c) Zeldes, H.; Livingston, R. *J. Chem. Phys.* **1966**, *45*, 1946.

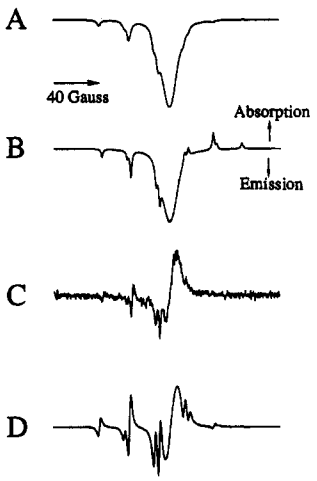

Figure 7. (A) Simulated spectrum of the *p*-butylbenzophenone/surface system **2** in a *n*-hexadecane slurry at 1.0 μs. (B) Simulated spectrum of *p*-but-1-en-4-ylbenzophenone in *n*-hexadecane solution at 1.0 μs. (C) First derivative of TREPR spectrum from surface attached *p*-butylbenzophenone in a *n*-hexadecane slurry at 1.0 μs (from Figure 5B). (D) First derivative spectrum of (A).

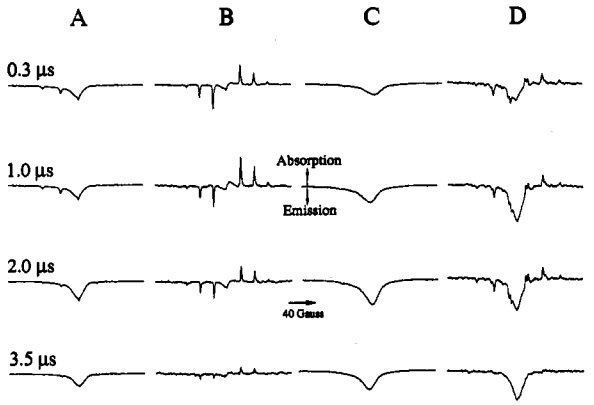

Figure 8. X-band time-resolved EPR spectra obtained at the delay times indicated. (A) Surface attached *p*-butylbenzophenone in a 2-propanol slurry. (B) *p*-But-1-en-4-ylbenzophenone in 2-propanol solution (gain × 10). (C) Surface attached *p*-butylbenzophenone in a *n*-hexadecane slurry. (D) *p*-But-1-en-4-ylbenzophenone in *n*-hexadecane solution (gain × 10, except at 0.3 μs, where the gain was × 5).

major change in the decay rate of radical **2c** in these two situations. In fact, strong signals from radical **2c** are observed at delay times beyond 8 μs in both solvent systems. In *n*-hexadecane (right half of Figure 8), the polarization magnitude on the surface is stronger than in free solution, but the decay rate of the ketyl radical EPR signal is about the same for both cases. If the decay is assumed to be mostly due to T_1 processes, we can infer that anchoring a radical of this size and chain length to the surface changes the effective viscosity by approximately the same amount as going from 2-propanol (1.77 cP) to *n*-hexadecane (3.34 cP).

Product analysis on the para-attached BP/2-propanol system was attempted by digestion of the silica in hot aqueous KOH (1 M), followed by cooling and extraction with diethyl ether. Low-resolution GC/MS results showed unreacted starting ketone with an –OH terminating the alkyl chain. Of the many other peaks, none showed definitively any expected photoproducts, and it may be that the harsh conditions required for the digestion process have caused further chemical reaction. Fragments consistent with diphenylmethanol were observed in several peaks, and the IR of the photoproducts showed a hydroxyl group peak at 3477 cm^{-1}. This indicates that the hydroxydiphenylmethyl radical center eventually reacts by hydrogen atom abstraction. The rate of this process would have to be very slow indeed as any new

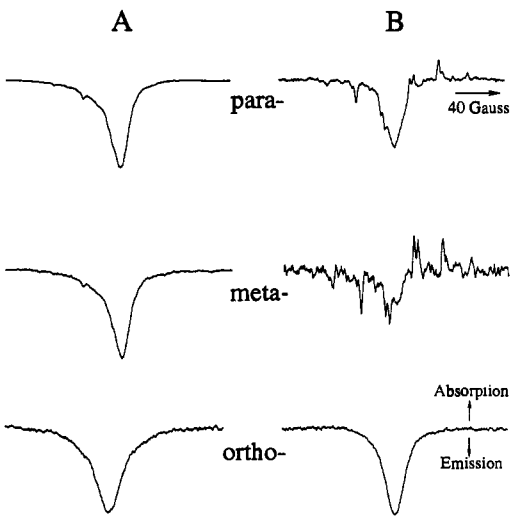

Figure 9. X-band time-resolved EPR spectra obtained at a 1 μs delay time during the flash photolysis of BP/silica system **2** in *n*-hexadecane slurries as a function of attachment position (ortho, meta, para). (A) Surface attached; (B) in free solution.

radical formed would be thermodynamically less stable than the bound radical.

The TREPR signals from the photochemistry shown in Scheme 1B are a strong function of the position of attachment to the phenyl ring of the ketone. Figure 9 shows a comparison of surface and solution TREPR spectra for the para-, meta-, and ortho-substituted ketones, respectively. There is very little difference in the surface spectra going from para to meta, and the minor decrease in the TM observed in free solution is probably due to a small difference in zero field splitting parameters between the two parent ketone triplet states. The ortho-attached ketone shows a signal that is broad and emissive, and the solvent radical signal is not present. A similar signal is observed for the ortho-attached ketone in free solution except that it has a narrower line width. This signal did not change with different solvents for either surface or free solution systems. Ortho-substituted BPs can undergo intramolecular H-atom abstraction reactions to produce 1,4-"photo-enol" type biradicals.[29] We have included a solution TREPR study of this ortho-alkylated benzophenone (alkyl and alkenyl) in a recent publication,[20] and based on the spectral width, time dependence, and strongly emissive character we have assigned it to the 1,4-biradical **2a** rather than the ketyl monoradical. This assignment is tentative at this point because the transient optical absorption decay data on structures of this type indicate that the chemical lifetimes are expected to be in the range of 100 ns. Here we see TREPR signals in solution and on the surface lasting for several microseconds. This discrepancy with the optical spectroscopy results is presently under further investigation.

Summary and Outlook

The TREPR spectroscopy of surface-bound radical pairs has been accomplished with satisfactory signal-to-noise ratios. The spin polarization mechanisms have been analyzed qualitatively, and all three (RPM, TM, and SCRP) have been shown to be strong functions of the effective viscosity the molecules experience at the solid/solution interface. For a four carbon alkyl chain tether, the change in effective viscosity for the BP radical **2c** from free solution is about a factor of 2. Major changes in spin–lattice relaxation times are also observed. Changes in the TM are easily rationalized in terms of increased rotational correlation times, and a small amount of SCRP polarization was observed for one system at very early delay times. Changes in the RPM were

(29) (a) Wagner, P. J.; Park, B.-S. *Org. Photochem.* **1991**, *11*, 227. (b) Wagner, P. J.; Meador, M. A.; Park, B.-S. *J. Am. Chem. Soc.* **1990**, *112*, 5199.

difficult to analyze because of the dominance of the TM. It is clear that tethering the parent ketones to the surface has a large effect on the TM. With the same tether length, minor solvent effects were observed for the RPM. In cases where reasonably strong RPM is observed, the polarization pattern predicted from a CIDEP model proposed by Monchick for two-dimensional diffusion appears but could conclusively be assigned to this mechanism because of interference from the TM. Extensions of these experiments to other surfaces and photochemical reactions are the subjects of present research.

Experimental Section

TREPR Methods. The time-resolved EPR experiments were performed at X-band using a JEOL, USA, Inc. JES RE-1X spectrometer system which has been modified for direct detection and fast time response as described in previous publications.[30] The radicals were generated within the microwave cavity of the spectrometer using an excimer laser (Lambda Physik LPX 110i, 308 nm, 15 ns fwhm, 200 mJ) firing at a repetition rate of 60 Hz. The TREPR signals were always found to be linear functions of the laser light intensity. Typical samples consisted of slurries of the ketone-modified silica (≈2 g per 50 mL of freshly distilled solvent), bubbled with dry nitrogen, continuously circulated through a 1 mm path length quartz flat cell centered in the microwave cavity which was a home-built copy of the Varian rectangular TE_{103} optical transmission cavity.

Characterization Methods. Gas chromatography/mass spectrometry (GC/MS) analyses were performed on a Hewlett-Packard 5890 GC automated with a 5971A MS instrument using a 12 m HP-1 capillary column. ^1H and ^{13}C NMR spectra were recorded on a Varian XL-400 spectrometer. Infrared spectra were obtained on a Bio-Rad FTS-7 spectrometer. For solution IR work a standard cell with NaCl windows and CCl_4 as solvent was used. For IR analysis of the surfaces the instrument was fitted with a diffuse reflectance accessory (Bio-Rad model DR) and run in the absence of solvent.

Solvents and Materials. Tetrahydrofuran was distilled from lithium aluminum hydride. Diisopropylamine and toluene were distilled from calcium hydride prior to use. Pyridine was distilled and stored over potassium hydroxide. Iodomethane, *n*-BuLi, hydrogen hexachloroplatinate(IV) hydrate (Aldrich), 2,4-dimethyl-3-pentanone (Aldrich), dimethylchlorosilane (Hüls), and allyl iodide (Janssen) were used as received. All compounds were purified by flash column chromatography carried out on 200–400 mesh, 60 Å silica gel (Aldrich). 10-Iodo-1-decene was prepared from 9-decen-1-ol (gift of Takasago Aroma Chemicals) according to literature procedures.[31] The linear aliphatic ketones were alkylated using standard enolate chemistry with lithium diisopropylamide as base and THF as the solvent, with addition of the appropriate alkyl or alkenyl iodide at −10 °C followed by warming to room temperature and stirring 3–6 h.

***p*-Butenylbenzhydrol.** A mineral oil suspension of Li (25% wt, 0.450 g, 0.016 mol) was placed in a dry 50 mL flask under N_2 and suspended in anhydrous diethyl ether (20 mL). To this was added dropwise 1.7 g of *p*-butenylbromobenzene (8.05×10^{-3} mol, synthesized from *p*-(bromo)-benzylbromide according to the method of Peterson et al.[32]) in diethyl ether (15 mL). The resulting mixture was allowed to reflux for 3 h and then cooled to room temperature. Benzaldehyde (0.85 g, 1 equiv) in diethyl ether (10 mL) was added dropwise and stirred for an additional 24 h. The reaction mixture was quenched with cold water (20 mL). The ether layer was washed with water, brine, and dried over anhydrous $MgSO_4$. Removal of the solvent gave 1.7 g (89%) of crude *p*-butenylbenzhydrol; GC/MS *m/e* 238 ($C_{17}H_{18}O$).

***m*-Butenylbenzhydrol** was synthesized as above from *m*-butenylbromobenzene in 60% yield; GCMS *m/e* 238 ($C_{17}H_{18}O$).

***o*-Butenylbenzhydrol.** To a stirred solution of *o*-(4-butenyl)benzaldehyde (4.9 g, 0.030 mol, synthesized from *o*-(butenyl)benzyl alcohol according to the method of Mariano[33] *et al.*) in diethyl ether (100 mL) at −40 °C was added phenylmagnesiumbromide (0.033 mol) dropwise. After the addition was completed, the solution was stirred at −40 °C (1 h), warmed to room temperature, stirred for an additional 24 h, and poured into a solution of NH_4Cl. The ether layer was washed with water and brine and dried over anhydrous $MgSO_4$. Purification by flash chromatography (10% ether/petroleum ether) gave *o*-butenylbenzhydrol (7 g, 96%); CG/MS *m/e* 238 ($C_{17}H_{18}O$).

***p*-Butenylbenzophenone.** To a stirred solution of pyridinium chlorochromate (3.26 g, 0.015 mols) in anhydrous CH_2Cl_2 (10 mL) was added Celite (6 g) and *p*-butenylbenzhydrol (2.4 g, 0.01 mols) in CH_2Cl_2 (10 mL) under a N_2 atmosphere. The reaction mixture was allowed to stir at room temperature (24 h), and the dark brown Celite was filtered off. The filtrate was concentrated and purified by column chromatography ($CHCl_3$) to give *p*-butenylbenzophenone (2.0 g, 84%) as a colorless oil: MS *m/e* 236 ($C_{17}H_{16}O$); ^1H (400 MHz, $CDCl_3$) δ = 2.39 (q, 2H), 2.78 (t, 2H), 5.01 (m, 2H), 5.84 (m, 1H), 7.27 (d, 2H), 7.45 (t, 2H), 7.56 (m, 1H), 7.76 (m, 4H); ^{13}C (400 MHz, $CDCl_3$): δ = 35.9, 36.2, 116.2, 129.0, 129.2, 130.8, 131.2, 133.0, 136.1, 138.3, 138.7, 147.8, 197.3; IR (neat) 3068, 2925, 1656 cm^{-1}; HRMS *m/z* calcd for $C_{17}H_{16}O$ 236.120115, found 236.119703.

***m*-Butenylbenzophenone** was synthesized as above by treating *m*-butenylbenzhydrol with pyridinium chlorochromate in 62% yield: MS *m/e* 236 ($C_{17}H_{16}O$); ^1H NMR (400 MHz, $CDCl_3$) δ = 2.38 (q, 2H), 2.76 (t, 2H), 4.99 (m, 2H), 5.83 (M, 1H), 7.38 (m, 2H), 7.46 (M, 2H), 7.58 (m, 3H), 7.77 (m, 2H); ^{13}C NMR (400 MHz, $CDCl_3$) δ = 35.1, 53.3, 115.4, 127.9, 128.3, 128.4, 130.0, 130.1, 132.4, 132.7, 137.7, 137.6, 137.8, 142.2, 197.0; IR (neat) 3060, 2922, 1655 cm^{-1}; HRMS *m/z* calcd for $C_{17}H_{16}O$ 236.120115, found 236.120422.

***o*-Butenylbenzophenone** was synthesized as above by treating *o*-butenylbenzhydrol with pyridinium chlorochromate in 82% yield: MS *m/e* 236 ($C_{17}H_{16}O$); ^1H NMR (400 MHz, $CDCl_3$) δ = 2.28 (q, 2H), 2.74 (t, 2H), 4.88 (m, 2H), 5.73 (m, 1H), 7.26 (m, 3H), 7.41 (m, 3H), 7.56 (m, 1H), 7.78 (m, 2H); ^{13}C NMR (400 MHz, $CDCl_3$) δ – 32.7, 35.6, 115.0, 125.3, 128.4, 128.6, 130.18, 130.22, 130.27, 133.1, 137.7, 138.4, 140.7, 198.5; IR (neat) 3061, 2930, 1662 cm^{-1}; HRMS *m/z* calcd for $C_{17}H_{16}O$ 236.120115, found 236.119722.

Surface Attachment Procedure. The ketone was attached to silicon oxide (PQ Corporation, BET surface area 366 $m^2\ g^{-1}$) surfaces (2 g of surface material per 4 mmol of ketone) in the following manner: The silica was pretreated by heating to 125 °C at 100 mTorr for 12 h. The ketone was pumped down for 12 h at 100 mTorr, and approximately 10 μg of chloroplatinic acid was added. The ketone and catalyst were slowly heated, and upon reaching 90 °C, 2 equiv of chlorodimethylsilane was added. The reaction mixture was refluxed (1h) at 40–55 °C to form the silyl chloride. Excess chlorodimethylsilane was separated from the keto-silyl chloride with vigorous stirring and vacuum evacuation for 1 h. The keto-silyl chloride, 150–250 mL of dry toluene, and 10 mL of pyridine were transferred to the flask containing the surface material under a dry nitrogen atmosphere. The reaction mixture was heated at 90–95 °C for 48 h. The workup of the surface attachment involved washes and filtration with 100 mL each of toluene, methanol, methanol/water (1:1), water, methanol, and diethyl ether. The diethyl ether wash showed no organic residue upon evaporation. Diffuse reflectance FTIR spectroscopy was used to identify the ketone attached to the surface. A strong signal in the carbonyl region from 1680–1690 cm^{-1} was seen for the aliphatic ketones, and an equally strong band at about 1655 cm^{-1} was seen for the benzophenones.

Acknowledgment. We thank J. A. Parker for assistance in the preparation of the manuscript and Dr. N. Miller of the PQ Corporation for a generous supply of purified and carefully sized silica gel. The donors of the Petroleum Research Fund, administered by the American Chemical Society, are gratefully acknowledged for support of this work through Grant No. 27431-AC4. We also thank the National Science Foundation for partial support through a 1993–1998 Young Investigator Award to MDEF (Grant No. CHE-9357108).

(30) (a) Forbes, M. D. E.; Peterson, J.; Breivogel, C. S. *Rev. Sci. Instrum.* **1991**, *66*, 2662. (b) Forbes, M. D. E. *J. Am. Chem. Soc.* **1993**, *97*, 3396.
(31) (a) Tipson, R. S. *J. Org. Chem.* **1944**, *9*, 235. (b) Longone, D. T. *J. Org. Chem.* **1963**, *28*, 1770.
(32) Peterson, P. E.; Chevli, D. M.; Sipp, K. A. *J. Org. Chem.* **1968**, *33*, 972.
(33) Ho, E.; Cheng, Y.-S.; Mariano, P. S. *Tetrahedron Lett.* **1988**, *29*, 4799.